

## Analysis of slim floor beams in fire: emphasis on the concrete constitutive models

### *Análise de vigas mistas de aço e concreto pertencentes a pisos de baixa altura em situação de incêndio: ênfase à influência dos modelos constitutivos do concreto*

F. M. ROCHA <sup>a</sup>  
fabio.rocha@usp.br

J. MUNAIAR NETO <sup>a</sup>  
jmunai ar@sc.usp.br

#### Abstract

The partial encasement of the steel beam in the concrete slab, as occurs on the slim floor constructional system, provides thermal protection which improves the behavior of the beam when exposed to fire. In order to evaluate the thermal and structural performance of the slim floor system, numerical models considering partially encased beams were developed using the FEM-based computational code DIANA. With respect to the constitutive models of the materials, it wasn't possible to represent the formulation presented in EUROCODE 4 or ABNT NBR 14323:2013, being replaced by alternative models. Numeric models were created at room and elevated temperature, which used some of the available options for the constitutive models of concrete and steel. Also, some parameters were analyzed such as: (a) the interaction rate between the steel and concrete and (b) the optimal combination of the thermal parameters, in order to obtain a more realistic response of the slim floor beams in fire.

**Keywords:** termostructural analysis, slim floor, partially encased beams, fire.

#### Resumo

A incorporação do perfil de aço na laje de concreto, como ocorre nos pisos mistos de baixa altura (slim floor), garante revestimento contra fogo ao aço, melhorando o desempenho da viga de aço frente às ações da corrosão e do incêndio. Com a finalidade de avaliar o desempenho térmico e estrutural desse sistema construtivo foram desenvolvidos modelos numéricos de vigas mistas de aço e concreto parcialmente revestidas com o uso do pacote computacional DIANA. No que diz respeito aos modelos constitutivos dos materiais, não foi possível representar as relações apresentadas no EUROCODE 4 e na ABNT NBR 14323:2013, por incompatibilidade dessas com o DIANA, sendo então adotados modelos alternativos. Em seguida, foram construídos modelos numéricos à temperatura ambiente e em temperatura elevada, contemplando as opções disponíveis e convenientes para as relações constitutivas do aço e do concreto. Também foram avaliados parâmetros como: (a) o nível de interação entre o aço e concreto, bem como (b) a melhor configuração para os parâmetros térmicos do concreto a fim de se obter uma resposta mais realista do comportamento das vigas pertencentes ao sistema slim floor em situação de incêndio.

**Palavras-chave:** análise termoestrutural, slim floor, vigas parcialmente revestidas, incêndio.

<sup>a</sup> Departamento de Engenharia de Estruturas, Escola de Engenharia de São Carlos, Universidade de São Paulo, São Carlos, SP, Brasil.

## 1. Introduction

It is well known that a steel cross-section with no fire protection subjected to high temperatures suffers a quick loss in its mechanical properties, mainly due to its high thermal conductivity. This imposes difficulties for an unprotected steel structure to achieve good fire resistance when exposed to high temperatures.

In the middle of the 19<sup>th</sup> century, structural elements made from the association of steel and concrete started to be used due to the protection against fire and corrosion the concrete provided to the structure (Ramos [1]). Presently, the steel and concrete composite structures have a considerable importance and acknowledgment, mostly because they result in structural systems which uses the benefits of both materials in an efficient way. In this context, Slim Floor structures (Figure 1) can be highlighted. This type of composite structure consists in the partial or complete incorporation of the steel profile in the concrete slab, reducing the total height of the beam and increasing the working height of the floor.

The partial incorporation of the steel profile in the concrete slab provides a protective coating, making the slim floor constructional system a good solution for the design of structures in fire and eliminating the use of additional fire-protective coatings.

The study of these cases can be performed through tests in furnaces, which are usually expensive and require a well-trained group of researchers, or through numerical analysis that simulates the complete structural element and its relevant parameters. Furthermore, a numerical analysis can provide results like stresses, strains and temperatures at any point of the structure. The cross section of a slim floor beam is composed of a great amount of concrete. Therefore, the Finite-element analysis program DIANA was chosen, which has been widely used for modeling reinforced concrete structures, mainly due to the available concrete smeared-crack models.

## 2. Methodology

To better understand the slim floor beam's structural behavior in fire, this paper reports a numeric study on the subject. All numeri-

cal analyses were performed using the computational code DIANA. A thermal-stress model in DIANA should be formed basically by two different domains: one that considers the heat transfer analysis (known as potential flow analysis in the program) and another for the structural analysis (which will be nonlinear, accounting for the temperature change effects). These two domains are overlapped, converting the results of the heat transfer analysis (temperatures) into input data in the structural analysis.

Hereafter are shown some of the most important aspects of the numerical modeling strategy and all considerations done during the development of a complete 3D thermal-stress finite element model. More details can be found in Rocha [2].

### 2.1 Considerations on the finite elements

Starting with the numerical model for the structural analysis of slim floor beams at room temperature developed in Ramos [1], which also used the software DIANA, the necessary modifications were made so that the model could perform a sequentially coupled thermal-stress analysis. The initial model, in the stress and strain domain, used the three-dimensional solid element CHX60 with 20 nodes and quadratic interpolation for the displacement and three degrees of freedom per node. In the contact region between the steel profile and the concrete a 16-node quadratic interface element CQ48I of three degrees of freedom was used.

The thermal-stress analysis in DIANA overlaps the heat and stress domains, therefore the finite elements chosen for the heat transfer analysis should be compatible with the ones previously described. The heat transfer elements HX8HT and IQ8HT (Figure 2) were used to represent the steel, concrete and the interface between elements, respectively. Element BQ4HT was used to model the convective and radiative heat transfer in the exposed surfaces. The heat transfer elements are linearly interpolated and their nodes are in the same position as the extreme nodes of the stress domain elements. The temperature of the intermediate edge nodes of the stress element is obtained by a linear interpolation of the corner's temperature.

The finite element model was first verified considering the heat transfer analysis using two and three-dimensional models. The model presented by Ramos [1] was reproduced and upgraded,

Figure 1 - Slim Floor Elements, Ramos (1)

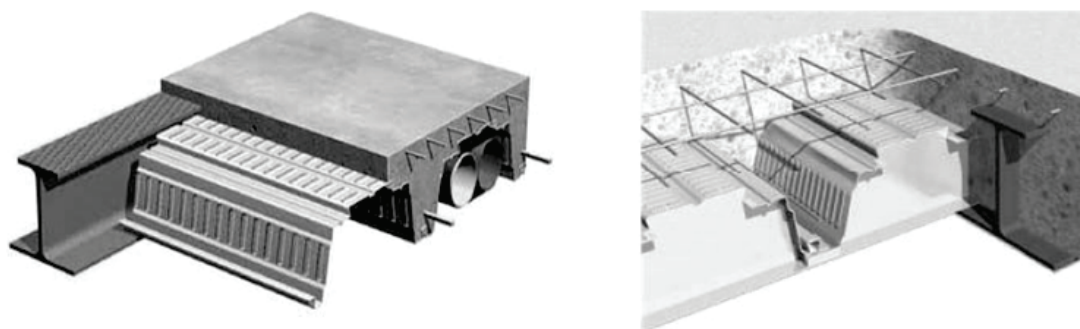
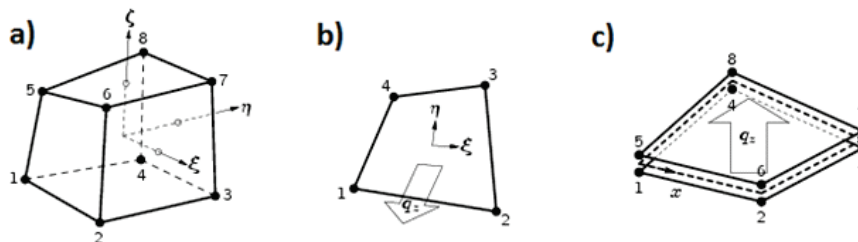


Figure 2 – Finite elements used during the thermal analysis:  
(a) HX8HT, (b) BQ4HT and (c) IQ8HT, Rocha (2)



and, as a last step, the sequentially coupled thermal-stress analysis was conducted and have its results were compared with the test results available in the literature.

During the verification of the heat transfer model, the performance using quadratic and linear interpolated finite elements and different meshes were evaluated, just to make sure that the use of a linear interpolated heat transfer finite elements would not cause any loss in the accuracy of the calculated temperatures. The results were compared with those provided in Regobello [3], Dong & Prasad [4] and Lawson *et al.* [5].

The model used the two symmetry axes of the beam, which resulted in the geometry shown in Figure 3. The displacements in the normal direction of the symmetry planes were fixed.

2.2 Considerations on the material

Due to DIANA'S limitations concerning the sequentially coupled thermal-stress analysis and the temperature-dependent constitutive models, the finite element model was tested at room temperature using different concrete constitutive models available in DIANA library. The same models were tested at high temperatures and validated using the test results provided in Lawson *et al.* [5]. As previously stated, some difficulties were faced in the representation of the constitutive models used in Ramos [1] considering

high temperatures, mainly due to the unavailability of functions and specific parameters that needed to be temperature-dependent. In the following topics the considerations related to the temperature-dependent constitutive models of the steel and the concrete will be addressed.

2.2.1 Considerations on the steel

In the reference model at room temperature presented in Ramos [1], the steel elastic perfectly-plastic stress-strain relationship with the yield point at 410 MPa was chosen to represent the steel behavior, associated with the von Mises yield criterion. However, EUROCODE 4 Part 1.2 [6] shows a specific temperature-dependent stress-strain curve for the steel (Figure 4). The EUROCODE 4 Part 1.2 [6] model was chosen to represent the steel behavior under fire conditions during DIANA thermal-stress analysis.

One of the main limitations of DIANA data input is that it is impossible to create multilinear temperature-dependent constitutive models, therefore, the models showed in EC4 [6] cannot be represented. In other finite-element-based analysis programs such as ANSYS and ABAQUS this function is available. Therefore, the EC4 [6] stress-strain relationship was implemented by a strain hardening material model implemented in DIANA, specifying the stress of the material related to each plastic strain and temperature. The von Mises yield criterion was also considered.

Figure 3 – Numeric model analyzed using two symmetry axes

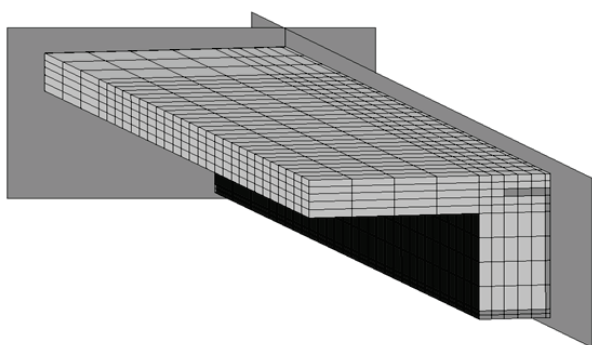
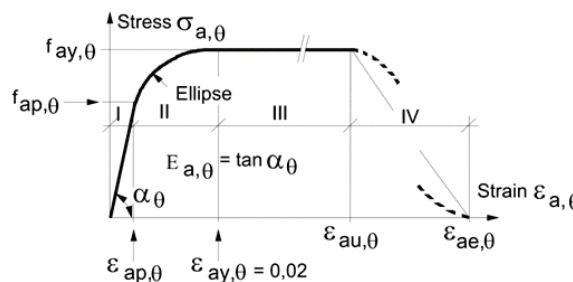
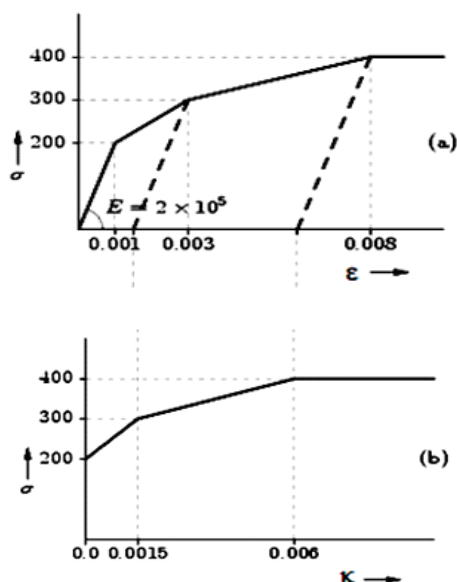


Figure 4 – Stress-strain relationship of the steel for elevated temperatures, EUROCODE 4 part 1.2 (6)



**Figure 5 – Method for obtaining the equivalent plastic strains from a stress-strain relationship, Rocha (2)**



The equivalent plastic deformation, represented by parameter  $\kappa_\theta$ , is obtained as shown in Figure 5, and the equation 1.

$$\kappa_\theta = \varepsilon_\theta - \sigma_\theta / E_{a,\theta} \tag{1}$$

Where

- $\kappa_\theta$  is the plastic strain at temperature  $\theta$ ;
- $\varepsilon_\theta$  is the total strain at temperature  $\theta$ ;
- $\sigma_\theta$  is the stress of the material at  $\theta$ ;
- $E_{a,\theta}$  is the Young's Modulus of the steel at temperature  $\theta$ .

**2.2.1 Considerations on the concrete**

EC4 [6] provides some considerations regarding the constitutive models of the tensioned and compressed concrete. However, as previously mentioned, it is impossible to represent the stress-strain temperature-dependent curves as a multilinear model, especially using the Total Strain Fixed Crack model.

Under these circumstances, the same constitutive models used in the reference model at room temperature developed in Ramos [1] were chosen for use. The parameters were assumed to be temperature-dependent and used the resistance reduction factors provided in the EC 4 [6] and the Young's Modulus reduction factors of the ABNT NBR 14323:2013 [7]. The *tensioned concrete* was represented by an exponential stress-strain curve (Figure 6a) and the fracture energy in the traction could assume different values at different temperatures. The elastic perfectly-plastic (Figure 6b) model was also tested.

To represent the *compressed concrete*, considering the Total Strain Fixed Crack models, DIANA has several stress-strain relationships implemented into its code (Figure 7). As a first attempt, the parabolic model (Figure 7g), which is the same as the one used in Ramos [1], was chosen. However, the DIANA data input for this model does not allow parameter  $G_c$  (fracture energy in compression) to be temperature-dependent and the value used in cold condition was adopted to all temperatures. Since the fracture energy also varies with the temperature, this assumption could not represent correctly the real behavior of the compressed concrete in fire, especially in the descending phase of the stress-strain curve.

Besides the parabolic constitutive relation, using the fracture energy ( $G_c$ ) constant, other two stress-strain relationships were tested: Thorenfeldt and the elastic perfectly-plastic models, shown in Figures 7c and 7b, respectively. The Thorenfeldt model was chosen mainly because its formulation does not depend on the fracture energy ( $G_c$ ) and requires only the compressive strength and the Young's modulus, which can be temperature-dependent. The elastic perfectly-plastic model was chosen due to its simple formulation, which results in a lower computational cost. Although this simplification resulted in a significant loss in the results precision. Concerning the thermal properties of the concrete, such as thermal conductivity and specific heat, some values recommended by EC4 [6] may lead to a conservative fire resistance of the composite beams.

In the case of the thermal conductivity, EC4 [6] shows two different formulae (Figure 8a), representing the upper and lower limits of the parameter. The upper limit is recommended, because the values were obtained during the study of steel and concrete composite structures. Regarding the concrete specific heat, EC4 [6] shows a peak between 100 and 200°C due to the heat absorption by the concrete's incorporated water (Figure 8b). The amplitude of the peak is defined by the moisture content of the concrete, which can range from 4 to 10%, assuming values of 2200 and 5600 J/kg°C, respectively. If there is no information about the concrete moisture content, 4% should be adopted.

The normative suggestions related to thermal conductivity and specific heat (peak related to 4% of moisture content and upper limit for conductivity) result, in some cases, in concrete temperatures higher than the ones obtained in tests, leading to a conservative

**Figure 6 – Constitutive models adopted for the tensioned concrete, Rocha (2)**

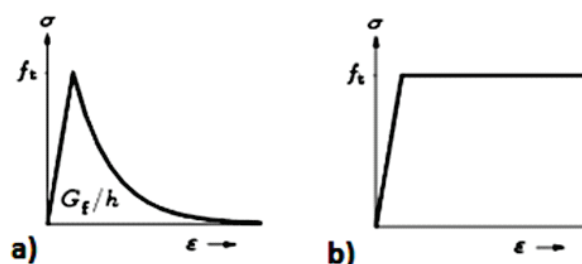
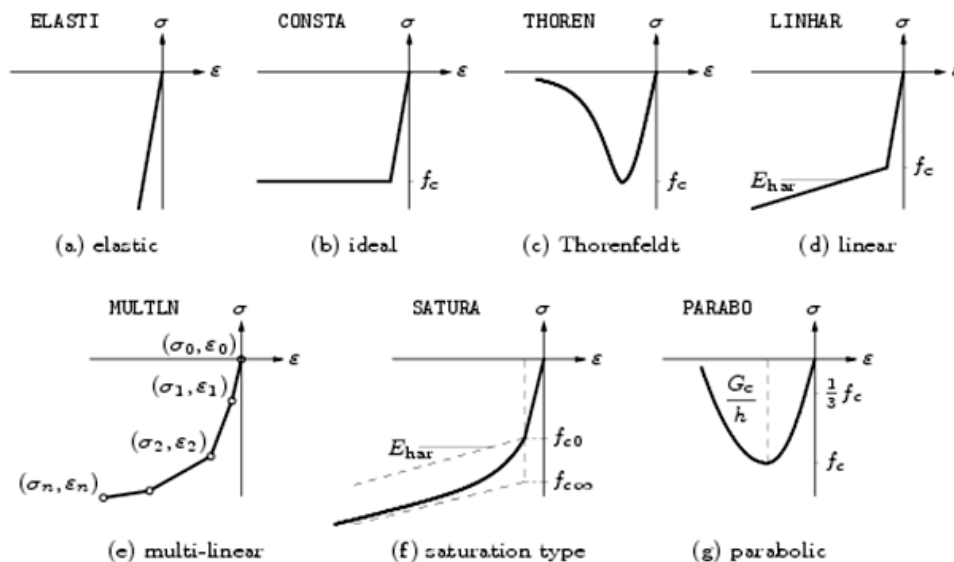


Figure 7 – Constitutive models available in DIANA to represent the compressed concrete, Rocha (2)



behavior, in which the structure fails before the real failure time. In the following analysis, the concrete thermal conductivity relationship was adopted as the average between the upper and lower limits of EC 4 [6], while the specific heat peak was adopted as 5600 J/kg°C, which corresponds to a 7% moisture content. The numerical results were compared with the ones from tests described in Lawson *et al.* [5]. The evaluation of the results is addressed in section 3.

2.2.3 Considerations on the steel/concrete interface

The contact region between the steel profile and the concrete en-

casement was modeled using interface elements, which has different purposes in the heat transfer and stress analysis. According to Makeläinen & Ma [8], in the heat transfer model a thermal conductance at the interface of 50 W/m²K is adopted. During the structural analysis, the interface was modeled by linear elastic parameters, which are the normal and shear stiffness moduli ( $D_{11}$  and  $D_{22}$ ) and whose values are 0,1 and 0,01 N/mm³, respectively. The interface stiffness values were suggested by Ramos [1].

2.3 Boundary conditions and loadings

In the heat flow analysis the boundary conditions were defined

Figure 8 – Thermal properties of the concrete: a) thermal conductivity; b) specific heat for different moisture contents (u), NBR 14323:2013 (7)

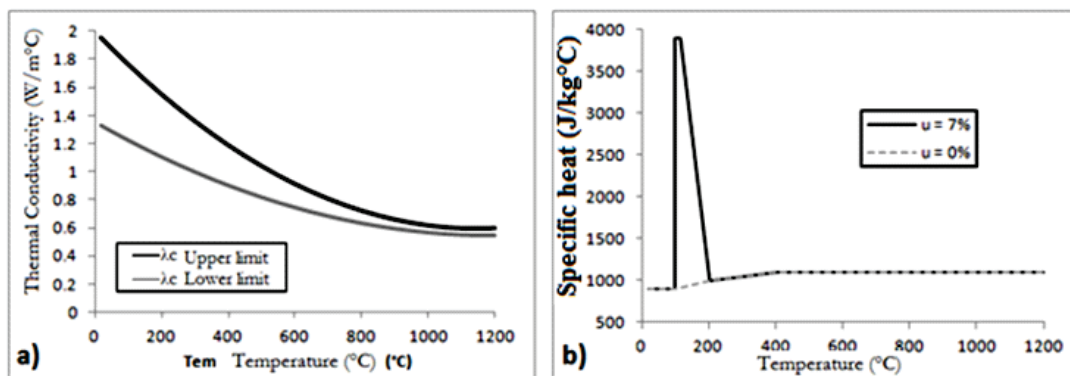


**Table 1 - Combination of the concrete parameters used in the thermal analysis, only the E07 hypothesis refers to the EUROCODE 4 Part 1.2 (6) prescriptions**

Hypothesis	Thermal conductivity	Specific heat peak	Emissivity	
			Concrete	Steel
E04	Average of upper and lower limits	3900 J/kg°C	0,4	0,6
E05	Average of upper and lower limits	5600 J/kg°C	0,5	0,5
E07	Lower limit	2200 J/kg°C	0,7	0,7

as regions in which the heat transfer may or may not occur. In all developed models, the upper surface of the cross-section is in contact with an environment without fire and modeled using only the convective heat transfer mechanism, using the convective coefficient ( $\alpha_c$ ) of 9 W/m<sup>2</sup>C (this value also accounts for the radiative heat transfer effect). The lower surfaces are exposed to the room in fire, and accounts for both convective and radiative heat transfer mechanisms. The convection is considered using  $\alpha_c$  equals to 25 W/m<sup>2</sup>C. Regarding radiation, EC 4 [6] suggests the use of a 0,7 emissivity, independently of the material in contact with the room in fire. Section 3.1 shows that a 0,7 emissivity results in higher cross-section temperatures than expected, leading to a conservative behavior of the beam.

Alternatively to the EC 4 [6] prescriptions, Makeläinen & Ma [8] and Ellobdy [9] considered 0,6 and 0,4 emissivities, for the fire-exposed surfaces made of steel and concrete, respectively.

Lastly, another situation was proposed, using the emissivity equals to 0,5 for all exposed surfaces. This value was suggested by the old version of the Brazillian design code ABNT NBR 14323 [7]. The

three hypotheses were compared, as shown in Table 1, to evaluate the one that best fits the test results presented in Lawson *et al.* [5]. The ISO 834:1999 [10] standard fire temperature *versus* time curve was considered in all analyses presented in this paper. The environment without fire was adopted a constant temperature of 20°C. The hypotheses shown in table 1 are named according to the emissivity value chosen.

Regarding the structural model, the adopted boundary conditions accounted for a simply supported beam, where the displacements in X and Y directions (The direction Z contains the longitudinal axis of the beam) were fixed at one support. Moreover, the two symmetry planes were considered, as shown in Figure 3, and the displacements in the normal directions of the plane were fixed.

### 3. Results

The thermal model was verified using the numerical and test results presented in Regobello [3], Lawson *et al.* [5] and Dong & Prasad [4]. The structural model was already been verified in Ramos [1].

**Figure 9 - Fire tests performed for the steel profiles: a) 280 ASB 100 and b) 300 ASB 153, Lawson *et al.* (5)**

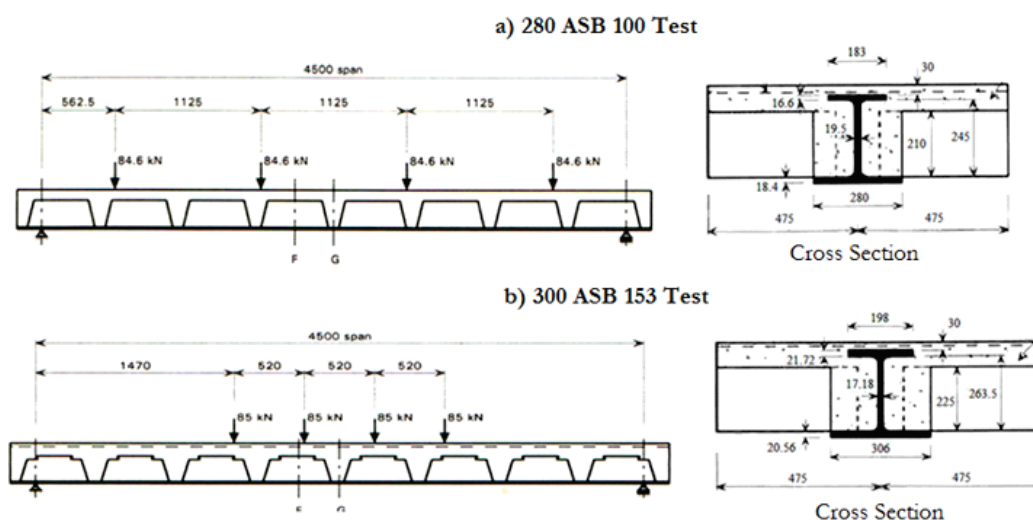


**Table 2 - Combination of the constitutive models in the analyzed cases**

Compressed concrete		Tensioned concrete	Steel
Elastic perfectly-plastic case	Elastic perfectly-plastic	Elastic perfectly-plastic	Elastic perfectly-plastic
Parabolic case	Parabolic	Exponential	EUROCODE 4
Thorenfeldt case	Thorenfeldt	Exponential	EUROCODE 4

**3.1 Thermal-stress model verifications**

There exist several ways to represent the concrete behavior in fire, regarding constitutive relations and other thermal parameters, such as thermal conductivity, specific heat and emissivity, shown in table 1. Thermal-stress models were performed for several combinations of parameters and constitutive models, aiming at the one that best represents the behavior of the slim floor beams in fire. The results provided in Lawson *et al.* [5] were used during the model verification. Such data are related to two bending fire tests in simply supported beams composed of the 280 ASB 100 and 300 ASB 153 asymmetric hot-rolled steel profiles. In both cases S355 steel and C30 concrete were used. The test configuration and the dimensions of the cross-section are shown in Figures 9a and 9b. The tests were performed in a sequential procedure, applying the mechanical load at first instance and then the thermal load, which varies in time. The heating proceeded until the stop criteria specified in BS476: Part 20 had been reached. In the first test, the heating stopped after 107 minutes, i.e. when the beam displacement had reached the limit of 225 mm (span/20). The second test proceeded until 75 minutes, when the maximum displacement rate had been reached. The displacement rate limit is not specified in Lawson *et al.* [5], but it is estimated to be close to 15 mm/min. As discussed in section 2.2.2, three constitutive relations were chosen to represent the compressed concrete in fire. Table 2 shows the three cases analyzed and the stress-strain relations adopted for the tensioned concrete and the steel. Those cases are named

according to the compressed concrete model adopted. The mid-span displacements of the beam versus exposure time for the standard fire are shown in Figures 10a and 10b, for both 280 ASB and 300 ASB tests. The three combinations of the constitutive models of Table 2 are shown in the graphs. All of them used the hypothesis of Table 1 (0,4 of concrete emissivity) for the thermal parameters. Although the displacements of the numerical results for the 280 ASB 100 profile were almost 15 mm greater than the ones measured experimentally, the modeling procedure represented the behavior beam in fire considerably well, during the whole exposure time. The best conformity with the reference results was achieved using the Parabolic and Thorenfeldt models. The elastic perfectly-plastic model led to greater displacements and against safety in both tests. In the 300 ASB profile models, the displacement runaway point was not reached. The results show that the parabolic model closely approaches the reference test data and that using the fracture energy constant over time in the parabolic model is acceptable. However, the thermal parameters used during the analysis are not the same as the ones recommended by EC 4 [6], which suggests a 0.7 emissivity for any material exposed to fire and an upper limit for the thermal conductivity and a specific heat peak of 2200 J/kg°C. Figure 11 shows the mid-span displacement versus exposure time curves for the E04 and E07 hypotheses of Table 1 for the models with the 280 ASB steel profile. As expected, the use of parameters which favor the temperature rise in the concrete results in a loss of the cross-section load-

**Figure 10 - Mid-span displacement versus exposure time for the steel profiles: a) 280 ASB 100 e b) 300 ASB 153**

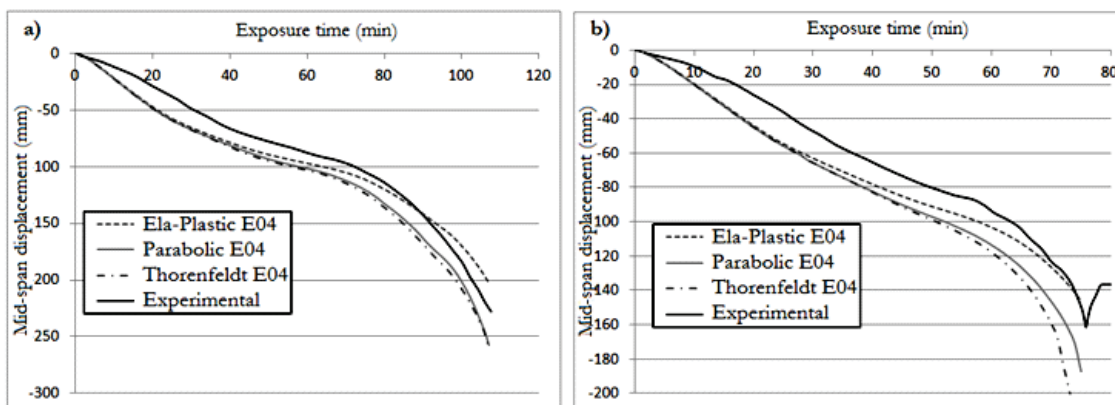
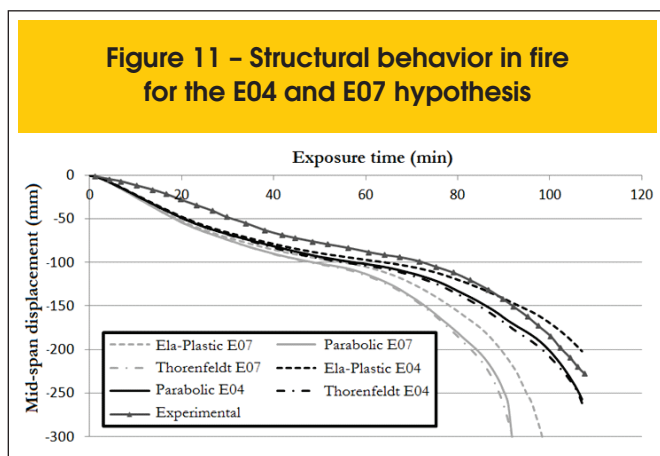


**Figure 11 – Structural behavior in fire for the E04 and E07 hypothesis**



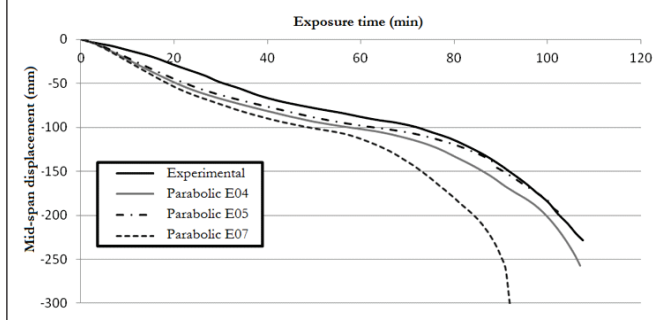
ing capacity, hence an earlier beam failure. Analyzing the results which used the parabolic constitutive model of the compressed concrete and the E07 hypothesis, the limit displacement (225mm) was reached with 88 minutes of fire exposure. In the E04 hypothesis, the limit displacement was reached after 104 minutes, which is much closer to the expected time of 107 minutes (test ending time). The same behavior was observed in the numerical analysis using the 300 ASB steel profile.

In the first 50 minutes of the fire exposure, the behavior was very similar in all cases (Figure 11), because the initial period is governed mainly by the thermal elongation of the materials. After this period, the loss of mechanical properties due to the fire action starts to govern the structural behavior until the failure time has been achieved.

The hypotheses described in Table 1 were created to analyze how the variability of the thermal parameters affects the structural behavior of the composite slim floor beams in fire. The analysis was performed because concrete is a material whose properties (thermal and mechanical) considerably vary depending on the amount of components and production.

The E05 hypothesis of Table 1 was created adopting a specific heat peak of 5600 J/kg°C, the maximum value prescribed by the EC 4 [6], which represents a 10% moisture content. A higher specific

**Figure 12 – Comparison of the thermal parameter hypothesis for the models with 280 ASB 100 steel profile and parabolic representation for the compressed concrete constitutive model**



heat peak of the concrete will lead to lower concrete temperatures, because the material will absorb more heat before its temperature changes. A 0.5 emissivity was used for all surfaces exposed to fire. Figure 12 shows the results for all hypotheses of Table 1, but only for the models which used the parabolic representation of the concrete and the 280 ASB steel profile. Although the results of the E05 hypothesis were closer to the expected final displacement of the test (225 mm), the displacement behavior changed considerably after 70 minutes of exposure, intercepting the reference curve and resulting in a final displacement smaller than the expected. The same characteristic was observed for other constitutive models. The results indicate the influence of a higher specific heat peak on the displacements behavior and the importance of considering the emissivity of the surface dependent on the material exposed to fire. The material-dependent emissivity is not considered in EC4 [6]. At the end of the results analysis, can be concluded that the E04 hypothesis leads to the best representation of the slim floor beams behavior in fire. This hypothesis was used in the following analysis.

### 3.2 Full interaction in fire

Another point of interest in the analysis of steel and concrete composite slim floor beams is the interaction rate between the steel profile and the concrete encasement. Most of the analytical methods presented in the normative codes evaluate the loading capacity of the structure in fire by the plastic analysis of the cross-section and consider only the full interaction between the steel and the concrete.

In the case of the slim floor beams, which have various steel-concrete contact surfaces with different interaction rates, the consideration of a full interaction in all these surfaces leads to higher resistive bending moments than the real ones. In previous analyses different interaction levels were considered: full interaction on the top surface of the beam's upper flange (due to the execution of grooves in this region during the profile fabrication); no interaction on the bottom surface of the upper flange (due to difficulties during concreting); partial interaction on the rest interface surfaces, using linear stiffness (axial and shear) parameters of  $D_{11}=0,1 \text{ N/mm}^2$  e  $D_{22} = 0,01 \text{ N/mm}^2$ .

Figures 13 and 14 show the mid-span displacement versus exposure time curves for the tests performed in Lawson *et al.* [5]. In both cases the E04 hypothesis of Table 1 was used.

**Figure 13 – Structural behavior in fire for the test with the 280 ASB 100 profile and full interaction**

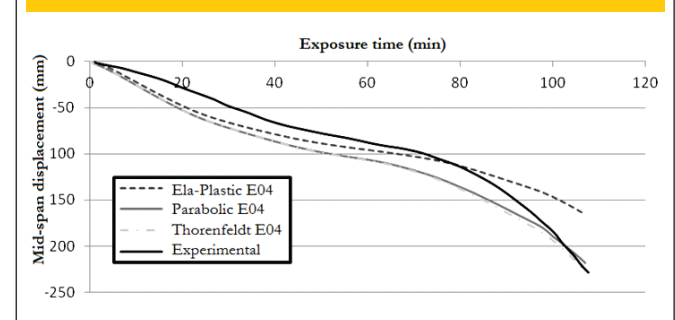
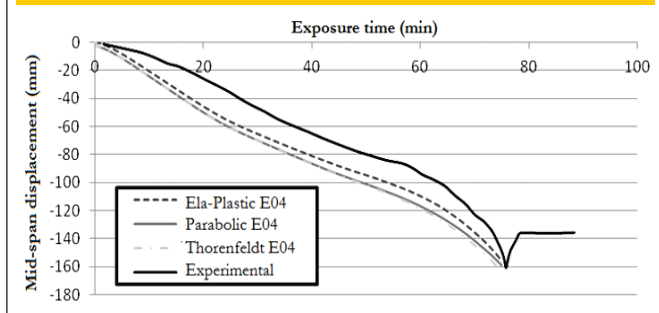


**Figure 14 – Structural behavior in fire for the test with the 300 ASB 153 profile and full interaction**



As expected, an enhancement was observed in the beams stiffness resulting in smaller displacements than those when a partial interaction was considered in some of the contact surfaces. Although the final displacements in the full interaction case were closer to the reference test results, the structural behavior changed considerably. This change is noted by the absence of a failure point at the final minutes of the analysis. The same happened in the partial interaction case, particularly on the 300 ASB 153 profile test.

The comparison of the models using the 280 ASB profile with partial and full interaction is shown in Figure 15. Concerning the mid-span displacement, the type of interaction between the steel and concrete, when the elastic perfectly-plastic model is used, and influence only after 60 minutes of fire exposure. The same happens only after 90 minutes when the parabolic or Thorenfeldt models were used.

These results show the strong influence of the concrete and its parameters on the thermal-stress response in the slim floor beams, especially when the structural element is near the failure point. This behavior occurs mostly because at the beginning of the heating process the steel beam is the part of the cross-section which contributes most to the composite section loading capacity. As the heating proceeds, the loading capacity of the steel profile decreases earlier than the concrete, mostly due to the fast heating of the bottom flange. Meanwhile, the concrete part of the section, which shows a milder temperature increase rate than the steel, maintains a more expressive share of its initial resistance, increasing its relative contribution to the loading capacity of the whole section at high temperatures.

#### 4. Conclusions

The analyses performed on DIANA, show that despite all the simplifications made on the concrete constitutive models, the computational code satisfactory represented the behavior of the steel and concrete composite slim floor beams in fire. Even considering the fracture energy constant through temperature, which was one of the main simplifications of the model, the parabolic stress-strain relationship was the one which represented best the reference experimental test results.

The thermal parameters used in the model can be represented in many ways and, depending on the designer's choice, they may result in considerable changes in the structural response of the

slim floor beams in fire. If all normative prescriptions are followed, the results become very conservative, reducing the fire resistance time in up to 20 minutes. Therefore a careful evaluation of some aspects, such as concrete moisture content and type of the slab used is required. The slab which uses a steel decking system has lower emissivity than the directly exposed concrete, leading to lower temperatures inside the cross-section.

Considering the full interaction between all steel-concrete contact surfaces results in enhancement of the fire resistance of the beam. The full interaction condition can be achieved in the real element, by making grooves or using shear connectors at the steel profile surfaces, resulting in a higher fire resistance of the slim floor beams in fire.

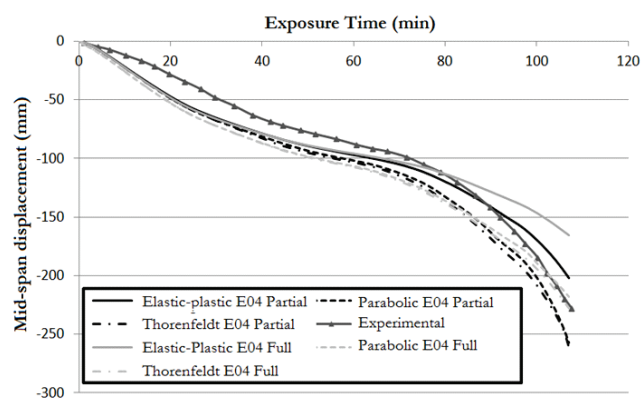
#### 5. Acknowledgments

The authors are indebted to the Brazilian National Council of Scientific Development – CNPq for the financial aid provided and the Department of Structural Engineering of the School of Engineering of São Carlos – SET/EESC/USP where the research was developed.

#### 6. References

- [01] RAMOS, A.L. Análise numérica de pisos mistos aço-concreto de pequena altura. 120p. Dissertação (Mestrado) – Escola de Engenharia de São Carlos, Universidade de São Paulo, São Carlos, 2010.
- [02] ROCHA, F. M. Modelos numéricos de vigas mistas de aço e concreto pertencentes a sistemas de pisos mistos de pequena altura em situação de incêndio. 269p. São Carlos. Dissertação (Mestrado) – Escola de Engenharia de São Carlos. Universidade de São Paulo, 2012.
- [03] REGOBELLO, R. Análise numérica de seções transversais e de elementos estruturais de aço e mistos de aço e concreto em situação de incêndio. 254p. São Carlos. Dissertação (Mestrado) – Escola de Engenharia de São Carlos, Universidade de São Paulo, 2007.

**Figure 15 – Comparison of the results using full and partial interaction for the models with the 280 ASB 100 steel profile**



- [04] DONG, Y.; PRASAD, K. Behavior of full-scale frames with slim floor slab construction under exposure in a fire resistance furnace. *Journal of fire protection engineering*, v.19, n.3, p. 197-220, 2009.
- [05] LAWSON, R. M.; MULLET, D. L.; RACKHAM, J. W. Design of asymmetric "Slimflor" beams using deep composite decking, Berkshire: Steel Construction Institute, SCI P-175, 106p, 1997.
- [06] EUROPEAN COMMITTEE FOR STANDARDIZATION. Eurocode 4 - Design of composite steel and concrete structures. Part 1-2: General rules – Structural Fire Design. EN 1994-1. Brussels, 2005.
- [07] ASSOCIAÇÃO BRASILEIRA DE NORMAS TÉCNICAS. Dimensionamento de estruturas de aço de edifícios em situação de incêndio – Procedimento. NBR 14323. Rio de Janeiro, Brasil, 2013.
- [08] MÄKELÄINEN, P.; MA, Z. Fire resistance of composite slim floor beams. *Journal of constructional steel research*, n.54, p.345-363, 2000.
- [09] ELLOBODY, E. Composite slim floor stainless steel beam construction exposed to different fires. *Engineering Structures*. v.36, p.1-13, 2012.
- [10] INTERNATIONAL STANDARD. Fire-resistance tests – Elements of building construct – Part 1: General requirements. ISO 834-1. Switzerland, 1999.